Optimizing the Step-by-Step Forming Processes for Fabricating a Poly(DL-lactic-*co*-glycolic acid)-Sandwiched Cell/Hydrogel Construct

Xiaohong Wang,[1,2] Shaochun Sui,[1] Chang Liu[3]

[1]*Key Laboratory for Advanced Materials Processing Technology, Ministry of Education and Center of Organ Manufacturing, Department of Mechanical Engineering, Tsinghua University, Beijing 100084, People's Republic of China*
[2]*Business Innovation Technology (BIT) Research Centre, School of Science and Technology, Aalto University, P.O. Box 15500, 00076 Aalto, Finland*
[3]*Department of Chemical Engineering and Technology, South China University of Technology, Guangzhou 510640, People's Republic of China*

Received 21 May 2010; accepted 20 July 2010
DOI 10.1002/app.33093
Published online 9 November 2010 in Wiley Online Library (wileyonlinelibrary.com).

ABSTRACT: A poly(DL-lactic-*co*-glycolic acid) (PLGA)-sandwiched cell/fibrin construct was fabricated to overcome the weak mechanical properties of cell/hydrogel mixtures. This construct was formed with a step-by-step mold/extraction method to generate a middle smooth muscle layer of natural blood vessels. A desired three-layer construct, as an integrated entity with optimized inner structures, was achieved by the control of the size of the molds, the concentration of the polymer systems, and the temperature of the extraction and polymerization processes. The constructs were fabricated with the following dimensions: length = 10–25 mm, diameter >2 mm, and wall thickness = 0.6–2 mm. Different microstructures in different layers of the sandwiched structure resulted in different functions. The pore structure in the inner PLGA and middle fibrin layers was beneficial for nutrient transference, whereas the solid structure without pores in the outmost surface of the outer PLGA layer could prevent fluid from leaking during *in vitro* culturing and *in vivo* implantation. This study showed that this can be a promising approach for the fabrication of synthetic-polymer-sandwiched viable cell/hydrogel constructs for wide potential application in complex organ manufacturing. © 2010 Wiley Periodicals, Inc. J Appl Polym Sci 120: 1199–1207, 2011

Key words: biocompatibility; bioengineering; biological applications of polymers; biopolymers; injection molding

INTRODUCTION

Organ manufacturing faces many challenges, including the isolation and expansion of multiple-cell lineages, the arrangement of assorted cells into the correct spatial organization, and the creation of the optimal microenvironments for the growth and differentiation of different cell types. The ability to create a vascular system is a significant step toward the goal for the manufacture of complex organs. Blood vessels are critical for maintaining cell viability during tissue growth. They induce structural organization and promote vascularization upon implantation.[1]

A smooth muscle component in the conduits can provide appropriate mechanical properties to withstand the fluid pressure and regulate the blood pressure. Over the past 50 years, creative physicians and scientists have developed various conduits for regenerating vascular tissue, especially vascular smooth muscle tissue.[2] Several strategies have been developed to overcome limitations on the regeneration of vascular smooth muscle tissue. However, the limited proliferative capacity of mature smooth muscle cells and the poor mechanical properties of the conduit scaffolds have thwarted previous attempts.[3] To obtain viable-order smooth muscle tissue, the supporting material should not only act as a mechanical support and geometrical guidance but also

Correspondence to: X. Wang (wangxiaohong@tsinghua.edu.cn).

Contract grant sponsor: National Natural Science Foundation of China/Research Grants Council of Hong Kong; contract grant number: 50731160625.
Contract grant sponsor: National Natural Science Foundation of China; contract grant numbers: 30970748, 30540060, and 30440043.
Contract grant sponsor: National High Tech 863 Grant; contract grant number: 2009AA043801.
Contract grant sponsor: Tekes Finnish Funding Agency for Technology and Innovation (as part of the project Bioman II); contract grant number: 40079/07.
Contract grant sponsor: Finland Distinguished Professor Program.
Contract grant sponsor: Beijing Municipal Science and Technology Commission; contract grant number: H060920050530.

provide a suitable macromolecular signal environment able to guide and direct *in vitro* tissue development.

Poly(DL-lactic-*co*-glycolic acid) (PLGA) is a kind of biological scaffold material with good mechanical properties, suitable pore sizes for cells to penetrate, and the ability to incorporate growth factors. PLGA has been widely used in cartilage tissue, adipose tissue, blood vessel, liver, and other tissue engineering. Fibrin, a major structural protein involved in wound healing, represents a sort of naturally derived scaffold material for the synthesis of autologous vascular systems. Fibrin hydrogel, with a degradation rate controllable by protease inhibitors, has been widely used in cell entrapment with a high cell seeding efficiency and homogeneous cell distribution during gelation.[4] However, the mechanical properties of a single fibrin hydrogel are not sufficient to withstand implantation in the vasculature.[5]

To overcome the shortcomings of single synthetic or natural polymers, we have developed several rapid prototyping techniques that enable the direct deposition of scaffold materials and cell/biomaterials at the right time, in the right position, and with the right amount. They can form three-dimensional (3D) complex architectures in a predesigned pattern in different environments.[6–12] On the basis of our cell-assembly technique, adipose stem cells (ADSCs) were assembled and induced into both endothelial cells and adipose cells in gelatin-based hydrogels.[13–16] Moreover, a PLGA-sandwiched fibrin/cell construct was fabricated with a step-by-step mold/extraction method. The mechanically stable PLGA was used as a supportive structural material to provide a well-defined microenvironment for the ADSCs to grow, migrate, and differentiate in the fibrin hydrogel.[17–20] The stem cells entrapped in the PLGA-sandwiched fibrin gel were induced into the smooth muscle cells and underwent pulsatile dynamic culturing *in vitro.* Compared with the static culture, the cells in the dynamic cultures aligned more uniformly throughout the middle layer of the construct. The main object of this study was to optimize the forming processes with different material systems.

EXPERIMENTAL

Material systems

PLGA/tetraglycol system

PLGA [lactic acid/glycolic acid (LA/GA) = 70/30, weight-average molecular weight = 100 kDa] was purchased from the Institute of Medical Polymers, Shandong, China. Tetraglycol was purchased from Sigma (St. Louis, MO, China); its chemical name was α-[(tetrahydro-2-furany) methyl]-ω-hydroxy-poly (oxy-1,2-ethyanediyl) α-[(tetrahydro-2-furyl) A base]-ω-hydroxy-poly(oxy-1,2-ethylene 2-yl), its molecular formula was $C_9H_{18}O_4$ (average), and its molecular weight was 190.24 (average). Bulk PLGA was dissolved in tetraglycol to form homogeneous solutions with concentrations of 5, 10, 15, and 20% (w/v).

Fibrin system

Fibrinogen and thrombin were purchased from Sigma. A 10% (w/v) fibrinogen solution was prepared by dissolution of the bulk fibrinogen in Dulbecco's modified Eagle's medium (Gibco, Santa Cruz, USA) without the addition of fetal bovine serum. Bovine thrombin (Sigma) was dissolved in phosphate-buffered saline to give a final concentration of 100 IU/mL.

Seeding cells

Rat ADSCs were isolated from the inguinal fat of Sprague Dawley (SD) rats. Adipose tissue was minced; this was followed by 45 min of 0.1% collagenase II digestion at 37°C to obtain the primary ADSCs. After culturing in Dulbecco's modified Eagle's medium supplemented with 10% fetal bovine serum for 12 h, the unstuck materials were removed, and the medium was changed every 3 days. The fifth-generation cells were used as seed cells after they were digested with 0.25% trypsin.

Extraction technique and pore size distribution of the single PLGA layer

A PLGA/tetraglycol solution (100 μL) was extracted with 1, 2, 3, or 4 mL of distilled water (extractant) at 25°C for 30 min. The distribution coefficient (K) and the extraction rate were calculated according to eq. (1). Each measurement was repeated three times:

$$\frac{C_{\text{water}}}{C_{\text{tetraglycol}}} = K \tag{1}$$

where Cwater is the concentration of water and Ctetraglycol is the concentration of tetraglycol.

After extraction, the unit area (100×100 μm^2) was selected from the images of scanning electron microscopy (SEM). IMAGE-PRO software was used to calculate the pore sizes and the pore size distributions. Three different areas were chosen for each image, and the calculation was repeated three times.

Step-by-step molds

An one-end-closed steel mold was designed to form the inner PLGA layer of the artificial constructs. This mold was divided into an inner part and an outer part. An open-ended polytetrafluoroethylene (PTFE)

mold was also designed to form the middle layer of the three-layer construct. This PTFE mold consisted of an upper part and a lower part. The two parts were put together to form go-through channels with different diameters (d values).

Viscosity (μ) measurement of the polymer solutions with different concentrations and forming temperatures

μ of the solution was measured with a disc method.[21] Briefly, a disc with a diameter of d was laid horizontally on the polymer solution with a thickness of h and a viscosity of μ. The disc was rotated at a speed of n (r/min) with a torque of M. As long as M was measured, μ of the fluid could be calculated. The values were proofread through multiple measurements of the water μ at room temperature (25°C). The μ values of the 5, 10, 15, and 20% (w/v) PLGA solutions at 25°C and the 10% (w/v) PLGA solution at 30, 40, 50, and 60°C were measured three times for each measurement.

Size control of the single PLGA layer

Two kinds of steel or PTFE molds with different lengths and d values were prepared before the experiments. The fabrication processes of the single tubular PLGA layer were described elsewhere.[17–20] We infused the 10% (w/v) PLGA/tetraglycol solution into the one-end-closed mold, making sure that the materials had full contact with the internal mold before the solvent tetraglycol was extracted. After extraction, the longitudinal shrinkage (a) of the tubular PLGA layer was calculated according to eq. (2):

$$a = \frac{l_0 - l}{l_0} \times 100\% \quad (2)$$

where l_0 is the length of the inner part of the one-end-closed mold and l is the length of the inner PLGA tubular structure after extraction. Similarly, calculation was carried out for the radial shrinkage with original wall thicknesses of 600, 800, 1000, and 1500 μm separately.

Impact of the extraction temperature on the pore structure of the tubular PLGA layer

The pore structures of the 10% (w/v) tubular PLGA layers after extraction at 4, 25, 40, and 60°C were observed with SEM.

Stability control of the cell/fibrin layer

Different concentrations, that is, 1, 2, 3, and 4% (w/v), of fibrinogen and thrombin solutions were prepared in phosphate-buffered saline. The polymerization times of fibrinogen at different temperatures were measured accordingly.

Cell compatibility with the fibrin hydrogel

Fibrinogen solutions with concentrations of 1, 2, 3, and 4% were prepared as described previously. ADSCs of the fifth generation were mixed with the solutions at a density of 1×10^6 cells/mL. The mixtures were placed in a six-well culture plate and polymerized with thrombin for further culture. The cell growth conditions were observed every 2 days.

RESULTS

Structure of the PLGA-sandwiched cell/hydrogel construct

As shown in Figure 1, the artificial construct with an interlayer of vascular tissue, made by the step-by-step mold/extraction method at room temperature (~ 25°C) in about 2 h, had a clear 3D structure. The dimensions of the three-layer construct, including the length, d, and thickness of the construct wall, could be controlled by the size of the molds. With the designed molds, different constructs were obtained with d values of more than 2 mm, lengths of 10–25 mm, and wall thicknesses of 600–2000 μm. The inner and outer layers for supporting layers were made of PLGA with different pore structures. The middle layer was a fibrin-encapsulated cell layer. A specific solvent evaporation method was used to make the nonpore outermost surface of the outer PLGA layer after the mold-forming and extraction processes. These three layers integrated closely and formed an organic entity. The pore structure in the inner PLGA had a certain penetration ability to ensure that the culture medium diffused into the middle cell/fibrin layer. The middle layer looked like a honeycomb network after freeze drying and provided accommodations for cells to grow, proliferate, migrate, and differentiate inside. The nonpore outmost surface of the outer PLGA layer could prevent liquid or blood from leaking during later *in vitro* or *in vivo* experiments.

Extraction effects

As shown in Figure 2, the distribution coefficients of the extractant water were in the range 147–152; this indicated that the extraction of the PLGA/tetraglycol system with water was easy to conduct. The extraction rate increased up to above 98%; that is, when 1, 2, 3, and 4 mL of water were used, the extraction rate increased (the values were 98.1 ± 0.86, 98.4 ± 0.72, 98.8 ± 0.65, and 99.2 ± 0.43%, respectively) as the extractant water volume increased, which

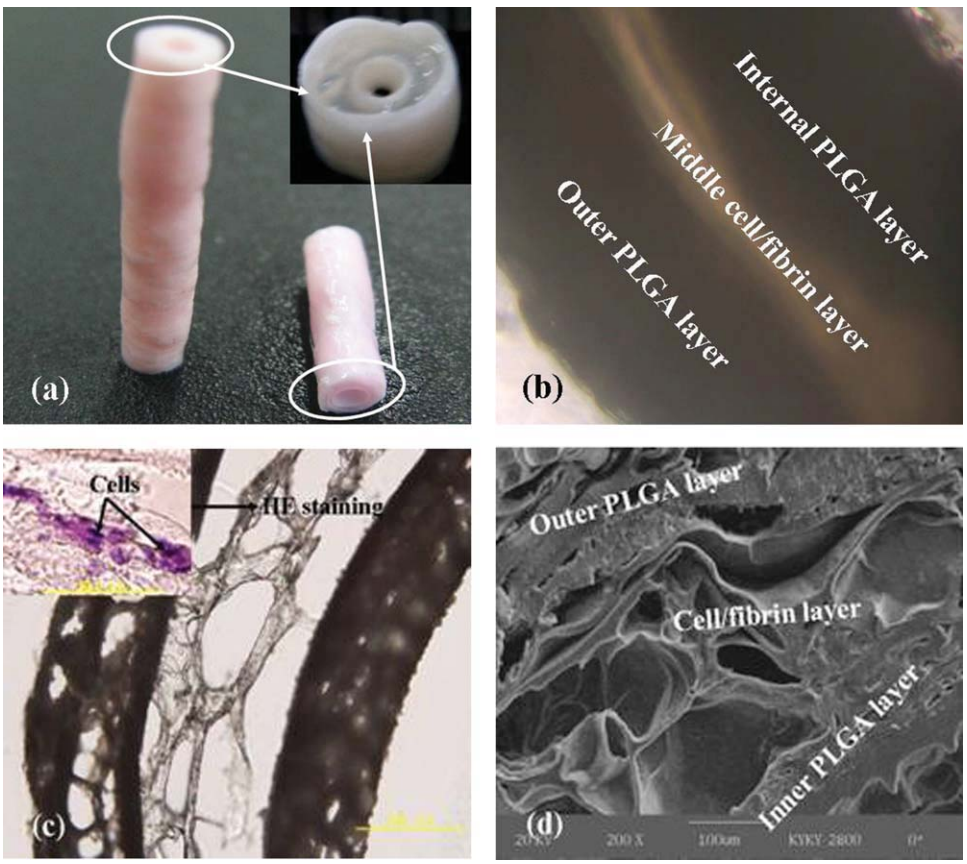

Figure 1 PLGA-sandwiched cell/hydrogel construct made by the step-by-step mold/extraction method: (a) the outlook of the three-layer constructs, (b) the three layers under an optical microscope, (c) freeze section with and without hematoxylin and eosin (HE) staining, and (d) a SEM picture showing the three layers integrated as an organic whole. [Color figure can be viewed in the online issue, which is available at wileyonlinelibrary.com.]

indicated that the PLGA/tetraglycol system had a high extraction effect in water.

Impact of the PLGA concentration on μ of the polymer solution

μ of the PLGA solutions increased exponentially with increasing concentration (i.e., when the concentrations of the PLGA solution were 5, 10, 15, and 20% (w/v), the μ values of the solution were 1.66 ± 0.02, 3.85 ± 0.53, 8.79 ± 1.04, and 17.16 ± 1.85 cp, respectively). μ of the 5% solution was too low for a stable forming process. The μ values of the 15 and 20% solutions were too high for the PLGA layers separate from the mold walls afterwards. The 10% solution had a suitable μ for the mold-forming processes with stable structures.

Impact of the forming temperature on μ

As shown in Figure 3, there were certain changes in the PLGA μ values with different concentrations at different temperatures. Among the different solutions, the μ values of the 5 and 10% solutions changed gently at different temperatures. The 5 and 10% PLGA solutions were suitable for the step-by-step forming and extraction experiments.

Size control over the PLGA-sandwiched cell/fibrin construct

The thickness of the three-layer construct was the total thickness of the inner PLGA layer, middle fibrinogen/cell layer, and outer PLGA layer. If the thickness of the construct wall was L and the thicknesses

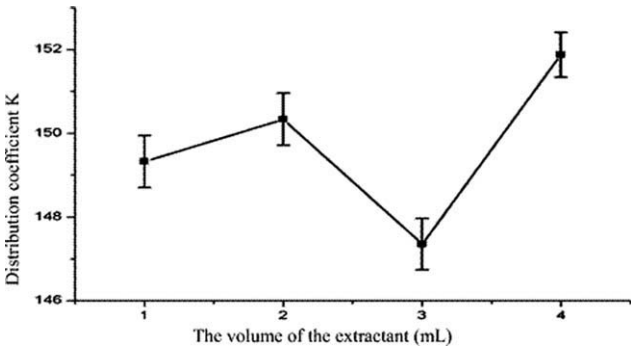

Figure 2 Distribution coefficients with different volumes of extractant water.

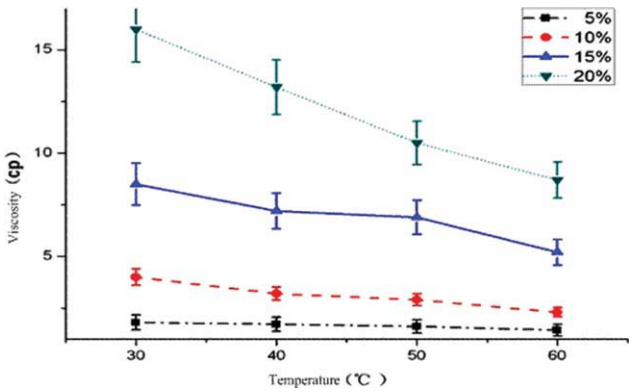

Figure 3 Temperature–μ curves of the PLGA/tetraglycol solutions with different concentrations at different temperatures. [Color figure can be viewed in the online issue, which is available at wileyonlinelibrary.com.]

of the three layers were l_1, l_2, and l_3 for the PLGA, fibrinogen/cell, and PLGA layers, respectively, the thickness of the whole construct wall could be calculated as

$$L = l_1 + l_2 + l_3$$

The length and d of the inner PLGA layer was determined by the one-end-closed molds. As expected, the length and inner d values of the PLGA-sandwiched cell/fibrin construct were consistent with the length and d values of the one-end-closed mold.

There was certain shrinkage of the inner PLGA layer after tetraglycol was extracted. The a values of the single PLGA layers with different lengths are shown in Table I.

Similarly, with tetraglycol extracted from the 10% PLGA/tetraglycol system, the PLGA layer gained a significant contraction in the radial direction. As shown in Table II, there was a radial shrinkage of about 30% after extraction. In addition, the outer PLGA layer had the same behavior with the inner PLGA layer.

Pore structures in the inner PLGA layer

An obvious pore structure was produced in the inner PLGA layer with a thickness of 180 μm after the extraction process. The transfer of tetraglycol started mainly from the interface of the PLGA/tetraglycol and the water systems and then from the outside surface to the inside surface. The pores formed in the inner PLGA layer had a clear orientation. Microscopic images indicated that the pores were relatively uniform with a d value of about 100 μm in the cross section of the inner PLGA layer.

TABLE I
a Values of the Single PLGA Layer with Different l_0 Values

l_0 (mm)	a (%)
10	1.8 ± 0.8
15	2.2 ± 1.0
20	3.6 ± 1.6
25	4.0 ± 2.2

TABLE II
Radial Shrinkage of the Single PLGA Layer

l_1 (μm)	Radial shrinkage (%)
600	34.3 ± 8.9
800	39.1 ± 11.2
1000	42.2 ± 11.4
1500	48.5 ± 12.3

The porosity and distribution of pore size was mainly determined by the concentrations of the PLGA/tetraglycol solutions. The inner PLGA layer formed at 25°C with 5% concentration formed small and messy pores in the 5% PLGA layer. In the 10% PLGA layer, the pores were large and relatively uniform. The d values of the pores in the 10% (w/v) PLGA layer were mainly in a range 25–45 μm. There were both large and small pores in the 15 and 20% PLGA layers. Particularly in the 20% PLGA layer, dense small pores were distributed in the walls of the large pores. Figure 4 shows the pore distribution in the inner tubular PLGA layers with different concentrations. These results indicate that relatively uniform pore distributions were achieved with the 10 and 15% PLGA solutions. According to the pore structure analyses on the inner PLGA layers with various concentrations, 10% PLGA/tetraglycol was chosen for the following experiments.

Impact of the extraction temperature on the pore structure of the single PLGA layer

The pore structures of the inner 10% PLGA layers at different extraction temperatures were observed with sample slices under a microscope (Fig. 5). It was

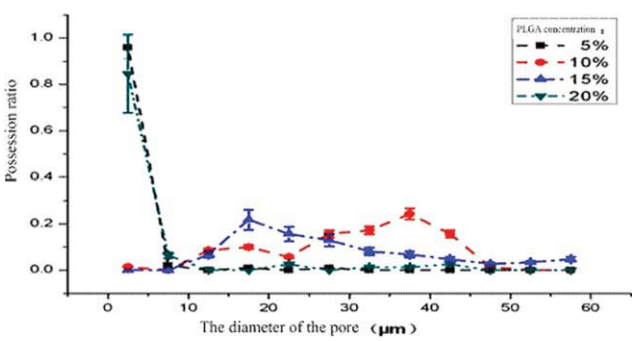

Figure 4 Distributions of the pore sizes in the inner PLGA layers with different concentrations. [Color figure can be viewed in the online issue, which is available at wileyonlinelibrary.com.]

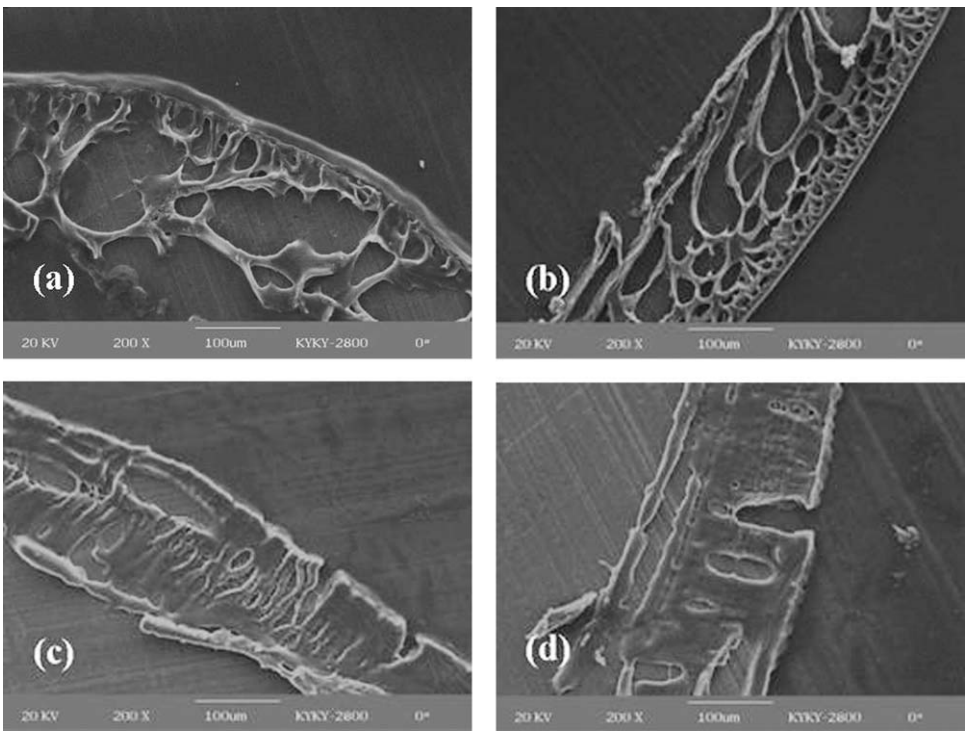

Figure 5 Pore structures of the inner 10% PLGA tubular layer formed at different extraction temperatures: (a) 4, (b) 25, (c) 40, and (d) 60°C.

clear that the pores got smaller and smaller and denser and denser with increasing temperature. In the 4°C sample slice, large and dispersive pores were uniformly distributed [Fig. 5(a)]. A stagger distribution of large and small pores occurred in the 25°C sample slice [Fig. 5(b)]. In the 40°C sample slice, small pores presented around the outer edge of the scaffold, and some middle and large pores presented in the inner edge [Fig. 5(c)]. Irregular pore structures appeared in the 60°C sample slice [Fig. 5(d)].

Stability of the cell/fibrinogen system

The time needed for polymerization of the fibrinogen solutions decreased correspondingly with decreasing fibrinogen concentrations, increasing thrombin concentrations, and polymerization temperatures. The thrombin concentration played the most important role. In addition, the polymerization times had a close relationship with the thickness of the cell/fibrin layer. Table III indicates the relationship between the thickness of the cell/fibrin layer and the times of polymerization. The thicker the cell/fibrin layer was, the more times it needed for polymerization.

Control over the pore structure of the cell/fibrin layer

The pore structure of the middle cell/fibrin layer was mainly determined by the fibrinogen concentration. Figure 6 shows the pore structures of the fibrin layer with concentrations of 1, 2, 3, and 4%. Significantly different pore structures occurred with different concentrations of the fibrinogen solutions. With increasing concentrations, the pores became denser and denser, smaller and smaller. When we compared the fibrin layer with the inner PLGA layer, the pores in the fibrin layer were relatively large and uniform. This was helpful for medium transmission in these two layers.

Cell compatibility with the fibrin hydrogel

More than 99% of the cells survived over the polymerization process in all of the samples (Fig. 7). Cells in the 4 and 3% fibrin hydrogels migrated out easily because the dense fibrin molecules affected the cell-to-cell connections [Fig. 7(a–f)]. After 5 days of culturing, obvious cell adhesion on the floor of the culture plate was observed. Little cell clusters were found in the high-concentration fibrin

TABLE III
Relationship Between the Polymerization Times and the Thickness of the Cell/Fibrin Layer

Polymerization times	Thickness of the cell/fibrin layer (μm)
1	196 ± 23
2	324 ± 34
3	456 ± 56

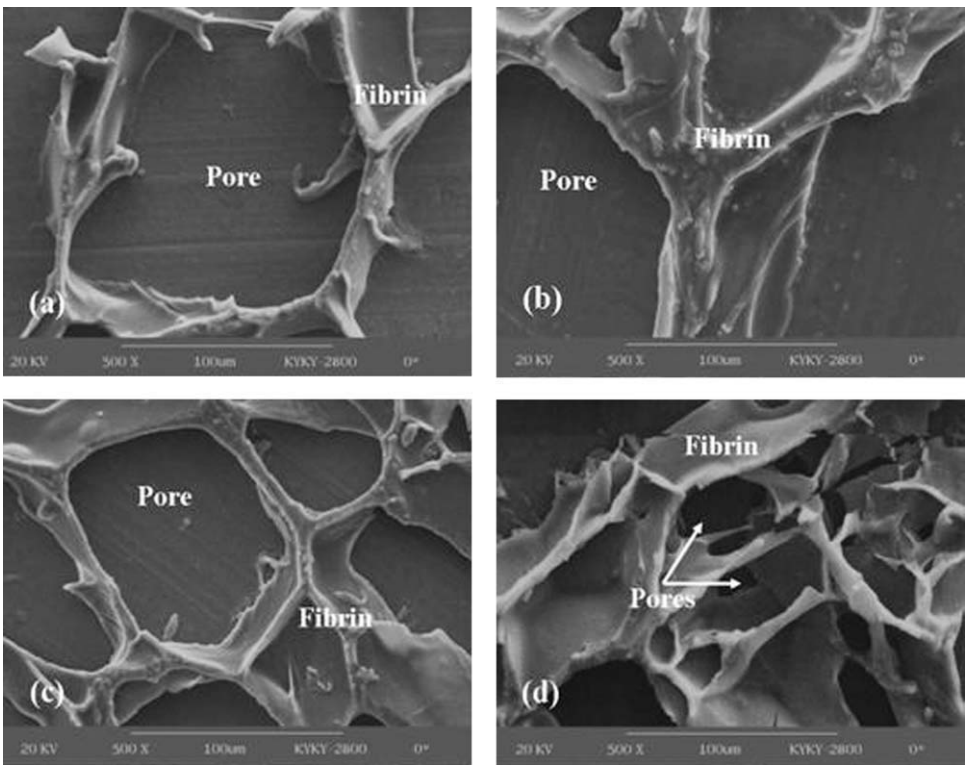

Figure 6 Pore structures of the fibrin layer with different concentrations of fibrinogen: (a) 1, (b) 2, (c) 3, and (d) 4% fibrinogen.

hydrogels. However, cells in the 2 and 1% fibrin hydrogels, especially in the 1% fibrin hydrogel, connected clearly with a lot of cell clusters and extended pseudopods after 5 days of culturing [Fig. 7(i,l)].

DISCUSSION

Organ manufacturing is an approach for alleviating donor shortages and provides an alternative treatment for organ failure. Complex organs have an abundant blood vessel supply; the branches of the blood vessels follow the connective tissue components of the muscle.[22] The lack of an adequate blood supply is an obstacle to complex organ manufacturing techniques. Different experimental methods have been developed for engineering functional smooth muscle tissues *in vitro* or *in vivo.* These include (1) the coculture of smooth muscle cells with endothelial cells and (2) the formation of vascular constructs from stem cells. However, most of the current available techniques fail to produce long-term satisfactory replacements because of four primary failure modes: acute thrombosis caused by the lack of a functional endothelium, restenosis caused by a chronic inflammatory responses, compliance mismatch caused by an improper smooth muscle layer, and susceptibility to infection.[23,24]

Artificial smooth muscle tissues need appropriate mechanical properties to fulfill their structural roles. Mechanical stimuli can clearly regulate the development of smooth muscle tissues.[25] To apply the mechanical stimuli to the assembled cells, the cell-laden constructs should be strong enough to endure harsh environments. Because of the inherent shortcomings, naturally derived polymers, such as fibrin and collagen, lack structural stability. They often cannot maintain their original structure during tissue development. It is difficult to design and engineer smooth muscle tissues with a predefined configuration and dimensions.[26] In our previous studies, we demonstrated that 3D smooth-muscle-like tissues could be fabricated by the culturing of ADSCs in PLGA-sandwiched cell/fibrin constructs. The phenotype of the cells was regulated by mechanical stimulation and growth factors.[17–20] Our model displayed a superphysiological bursting pressure, and the mechanical properties of the constructs could be modulated by the polymer concentration. As to materials applied for tissue regeneration, porosity is another vitally important parameter for cell communication and nutrition transport. In this research, we, therefore, optimized the step-by-step mold/extraction fabrication processes for good macrostructures and microstructures of the inner PLGA and middle cell/fibrin layers.

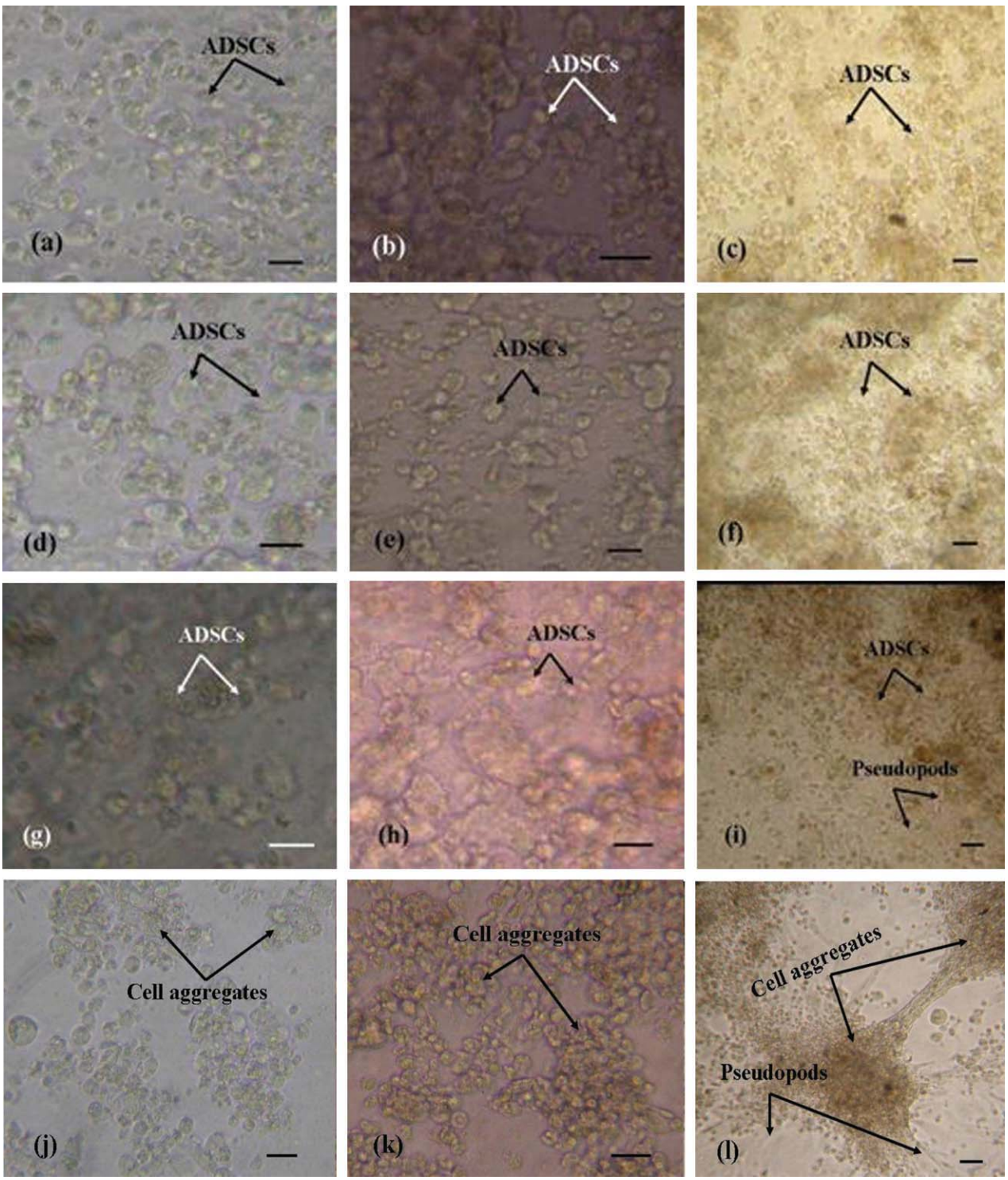

Figure 7 ADSC compatibilities with the fibrin hydrogels at different concentrations: (a) 4% fibrin after 1 day of culturing, (b) 4% fibrin after 3 days of culture, (c) 4% fibrin after 5 days of culturing, (d) 3% fibrin after 1 days of culturing, (e) 3% fibrin after 3 days of culturing, (f) 3% fibrin after 5 days of culturing, (g) 2% fibrin after 1 day of culturing, (h) 2% fibrin after 3 days of culturing, (i) 2% fibrin after 5 days of culturing, (j) 1% fibrin after 1 day of culturing, (k) 1% fibrin after 3 days of culturing, and (l) 1% fibrin after 5 days of culturing. Scale bars in the images represent 20 μm. [Color figure can be viewed in the online issue, which is available at wileyonlinelibrary.com.]

We demonstrated that the synthetic polymer PLGA could be prepared in tetraglycol solvents with different concentrations as a main factor determining the forming process of the three-layer constructs. The overall size of the PLGA-sandwiched cell/fibrin construct, including the length, *d*, and thickness of the wall, was mainly determined by the predesigned molds. Therefore, mold design was a key step in

this fabrication strategy. Parameter control was another important issue in the forming processes. The polymer concentration and the extraction temperature were two main factors that influenced the pore structures of the inner PLGA layer. A relatively uniform pore size and distribution appeared in the inner PLGA layer with a 10% concentration.

Because there were two different material systems in the PLGA-sandwiched cell/hydrogel construct, the relationship between the two systems had a great influence on the physical and biological performance of the entire construct. Figure 1(d) shows the close integrations between the PLGA and cell/fibrin layers. This combination was formed during the three-step mold-forming processes and was affected by the extraction and polymerization processes. Excellent integration between the three porous layers will be a very important issue in our further studies.

Fibrinogen is a water-soluble material with a high rate of water absorption. In this study, the fibrin hydrogel worked not only as the basic carrier of the seeding cells but also as the provider of the nutrition medium. The main factor influencing the forming stability of the cell/fibrin layer was the polymerization process with thrombin after mold shaping. After polymerization, the cell/fibrinogen system changed from the sol state into the gel state. This transformation process could be controlled by the fibrinogen and thrombin concentrations and by the polymerization temperature. As shown in Figure 6, the honeycomb-like pore structure was mainly determined by the fibrinogen concentration. These micropore structures could guarantee the cells to grow, proliferate, and differentiate well inside, which ensured cell-to-cell connections [Fig. 7(l)].

The cell compatibility of the fibrin hydrogel showed vital influence on the cell states afterward. Cell compatibility experiments showed that cells in the low-concentrations 1 and 2% fibrin hydrogels grew well with obvious connections. The reasons may have been that when the fibrinogen concentration was too high, the cells were encapsulated in the polymer molecules and cell-to-cell connections were greatly limited. However, when the fibrinogen concentration was too low, it was hard for the cell–polymer mixture to form a stable structure. The value of 1% fibrinogen was selected as the optimal middle-layer scaffold material. With this fibrin hydrogel, the metabolites of cells could be discharged in a timely manner, and the culture medium could be transported easily.

CONCLUSIONS

We have reported an optimization process created by the construction of a PLGA-sandwiched cell/hydrogel construct with a step-by-step mold/extraction method. The overall length and *d* values of the three-layer construct were mainly decided by the size of the predesigned molds. The pore structures of the inner PLGA layer were mainly controlled by the PLGA concentrations and the extraction temperatures. The pore structures and stabilities of the middle cell/fibrin layer were mainly controlled by the fibrinogen and thrombin concentrations and the fibrin hydrogel thickness. With carefully selected parameters, a desired three-layer construct with a predesigned configuration and functions was achieved. This approach can provide a new method for generating vascular smooth muscle tissue.

References

1. Niklason, L. E. Science 1999, 286, 1493.
2. Mitchell, S. L.; Niklason, L. E. Cardiovasc Pathol 2003, 12, 59.
3. McKee, J. A.; Banik, S. S. R.; Boyer, M. J.; Hamad, N. M.; Lawson, J. H.; Niklason, L. E.; Counter, C. M. EMBO Rep 2003, 4, 633.
4. Ye, Q.; Zünd, G.; Benedikt, P.; Jockenhoevel, S.; Hoerstrup, S. P.; Sakyama, S.; Hubbell, J. A.; Turina, M. Eur J Cardiothorac Surg 2000, 17, 587.
5. Aper, T. M.; Teebken, O. E.; Steinhoff, G.; Haverich, A. Eur J Vasc Endovasc Surg 2004, 228, 296.
6. Xu, W.; Wang, X. H.; Yan, Y. N.; Zhang, R. J. J Bioact Compat Polym 2008, 23, 103 (featured by *Nature China,* May 3, 2008).
7. Xu, W.; Wang, X. H.; Yan, Y. N.; Zhang, R. J. J Bioact Compat Polym 2008, 23, 409.
8. Xu, W.; Wang, X. H.; Yan, Y. N.; Zheng, W.; Xiong, Z.; Lin, F.; Wu, R. D.; Zhang, R. J. J Bioact Compat Polym 2008, 22, 363.
9. Yan, Y. N.; Wang, X. H.; Pan, Y. Q.; Liu, H. X.; Cheng, J.; Xiong, Z.; Lin, F.; Wu, R. D.; Zhang, R. J.; Lu, Q. P. Biomaterials 2005, 26, 5864.
10. Wang, X. H.; Yan, Y. N.; Pan, Y. Q.; Xiong, Z.; Liu, H. X.; Cheng, J.; Liu, F.; Lin, F.; Wu, R. D.; Zhang, R. J.; Lu, Q. P. Tissue Eng 2006, 12, 83.
11. Cui, T. K.; Yan, Y. N.; Zhang, R. J.; Liu, L.; Xu, W.; Wang, X. H. Tissue Eng Part C 2009, 15, 1.
12. Wang, X. H.; Yan, Y. N.; Zhang, R. J. Trends Biotechnol 2007, 25, 505.
13. Li, S. J.; Xiong, Z.; Wang, X. H.; Yan, Y. N.; Liu, H. X.; Zhang, R. J. J Bioact Compat Polym 2009, 24, 249.
14. Yao, R.; Zhang, R. J.; Yan, Y. N.; Wang, X. H. J Bioact Compat Polym 2009, 24, 5.
15. Sui, S. C.; Wang, X. H.; Liu, P. Y.; Yan, Y. N.; Zhang, R. J. J Bioact Compat Polym 2009, 24, 473.
16. Wang, X. H.; Yan, Y. N.; Zhang, R. J. Tissue Eng Part B 2010, 16, 189.
17. Wang, X. H.; Sui, S. C.; Yan, Y. N.; Zhang, R. J. J Bioact Compat Polym 2010, 25, 229.
18. Wang, X. H.; Sui, S. C. Artificial Organs, in press.
19. Wang, X. H.; Mäkitie, A. A.; Paloheimo, K.-S.; Tuomi, J.; Paloheimo, M.; Sui, S. C.; Zhang, Q. Q. Mater Sci Eng C, submitted.
20. Wang, X. H.; Mäkitie, A. A.; Paloheimo, K.-S.; Tuomi, J.; Paloheimo, M.; Sui, S. C. Adv Polym Technol, submitted.
21. Du, Z. X.; Hu, Y. F.; Zhang, S. Z. Colliery Engine 2006, 27, 1071.
22. Buckingham, M. Curr Opin Genet Dev 2001, 11, 440.
23. Veith, F. J. J. Vasc Surg 1986, 3, 104.
24. Seeger, J. M. Am Surg 2000, 66, 166.
25. Martin, I.; Wendt, D.; Heberer, M. Trends Biotechnol 2004, 22, 80.
26. Kim, B.-S.; Mooney, D. J. J Biomed Mater Res 1998, 41, 322.